Elastic and total cross sections for electron-carbon dioxide collisions in the intermediate energy range

1999 J. Phys. B: At. Mol. Opt. Phys. 32 4373

(http://iopscience.iop.org/0953-4075/32/17/318)

J. Phys. B: At. Mol. Opt. Phys. **32** (1999) 4373–4388. Printed in the UK PII: S0953-4075(99)03202-2

Elastic and total cross sections for electron–carbon dioxide collisions in the intermediate energy range

I Iga†, M G P Homem‡, K T Mazon‡ and M-T Lee†

† Departamento de Química, Universidade Federal de São Carlos, 13565-905, São Carlos, SP, Brazil

‡ Departamento de Física, Universidade Federal de São Carlos, 13565-905, São Carlos, SP, Brazil

Received 6 April 1999, in final form 21 June 1999

Abstract. In this work, we report on a joint theoretical and experimental investigation on electron–CO_2 collisions in the intermediate energy range. More specifically, the elastic differential, integral and momentum transfer cross sections as well as the grand total (elastic + inelastic) cross sections in the 30–500 eV energy range are calculated and reported. A complex optical potential consisting of static, exchange, correlation–polarization plus absorption contributions is used for the description of the electron–molecule interaction. The Schwinger variational iterative method combined with the distorted-wave approximation is applied to calculate the scattering amplitudes. In addition, experimental absolute elastic differential cross sections generated using the relative flow technique are reported in the 100–400 eV range. Comparison between the calculated results and present measured data and also existing experimental and theoretical results is encouraging.

1. Introduction

Electron collision with CO_2 is one of the most fundamental processes in planetary atmospheres, gaseous discharge and radiation interaction with matter. Therefore, it is not surprising that a large number of theoretical and experimental studies of e^-–CO_2 scattering have been reported over recent decades. On the experimental side, for instance, grand total (elastic + inelastic) cross sections (TCS) were measured over a wide energy range by several authors (Ferch *et al* 1981, Hoffmann *et al* 1982, Kwan *et al* 1983, Sueoka and Mori 1984, Szmytkowski *et al* 1987). More recently, a new set of cross sections including momentum transfer were determined by Nakamura (1995) via a swarm experiment. On the other hand, although elastic electron–CO_2 collisions were also investigated extensively (Shyn *et al* 1978, Register *et al* 1980, Kanik *et al* 1989, Tanaka *et al* 1998), most of the measurements on elastic differential and integral cross sections (DCS and ICS) were performed at incident energies up to 100 eV. Above that energy, experimental data on elastic DCS are scarce. Bromberg (1974) reported elastic DCS at 300, 400 and 500 eV in the 2°–45° angular range. Lately, DCS, ICS and also momentum transfer cross sections (MTCS) for elastic electron–CO_2 collisions were reported by Iga *et al* (1984) at 500, 800 and 1000 eV incident energies. On the theoretical side, the situation is rather similar. Earlier calculations for elastic electron–CO_2 collisions were reported by Morrison *et al* (1977), Onda and Truhlar (1979), Collins and Morrison (1982) and Lucchese and McKoy (1982). Despite some more elaborate calculations which were also reported recently (Takekawa and Itikawa 1996, Gianturco and Stoecklin 1996, Gianturco and Lucchese 1996, Tanaka *et al* 1998), the energy of incident electrons covered in those investigations did not exceed 100 eV. At higher energies, the only two cross

0953-4075/99/174373+16$30.00

section calculations for elastic electron–CO_2 collisions were reported by Lynch *et al* (1979) and Botelho *et al* (1984). However, very simple theoretical models were applied in their works.

It is well known that absorption effects (Joachain 1983) play an important role in electron–molecule scattering in the intermediate energy range (from ionization threshold to a few hundred eV). Although the main features of these effects are known, taking them into account in an *ab initio* treatment of electron–molecule scattering is a very difficult task. For instance, close-coupling calculations would have all discrete and continuum open channels included in the open-channel P-space, which would make the calculations computationally infeasible. In view of these difficulties, the use of the model absorption potential seems at present to be the only practical manner in which to carry out calculations on electron–atom and electron–molecule collisions. Indeed, several model absorption potentials of both empirical (McCarthy *et al* 1977, Green *et al* 1981, Thirumalai and Truhlar 1982) and non-empirical (Joachain *et al* 1977, Staszewska *et al* 1983) natures for electron–atom scattering have been proposed for more than 15 years. Among these model potentials, the quasi-free scattering model (QFSM) proposed by Staszewska *et al* (1983) is particularly interesting. The QFSM is derived non-empirically to reproduce the absorption probability per unit time for an electron passing through a free-electron gas, where the electron–electron absorption cross sections are calculated using the Pauli-allowed binary-encounter approximation. The target is modelled locally as a free-electron-gas (FEG) with Fermi momentum k_F depending on the density. Lately, the QFSM was modified empirically by Staszewska *et al* (1984) in order to introduce some target properties, such as ionization potentials and mean excitation energies, into the collisional dynamics. Two of these modified versions, namely versions 2 and 3 of the QFSM, have been the most successful. Unlike other empirical models (McCarthy *et al* 1977), the use of semiempirical QFSM versions does not require any parameters to be adjusted for a given target and for a given incident energy. Therefore, it is easy to use, and can provide cross sections for predictive purposes, rather than just for correlation and interpolation of a pre-existing database. For instance, the elastic DCS calculated by Staszewska *et al* (1984) using QFSM version 3, for the rare gases He, Ne and Ar over a wide energy range, are in very good agreement when compared with experimental data.

Because of its simplicity, it would be highly desirable if the QFSM could be applied successfully for electron scattering from molecular targets. Unfortunately, the applicability in cross section calculations for electron–molecule collisions has not yet been tested sufficiently. Among the few applications of QFSM for molecule targets reported in the literature, the calculations were performed either using only the spherical part of the interaction potential (Jain 1986, Jain and Baluja 1992) or made use of the additivity rule (Jiang *et al* 1995). Very recently, Lee and Iga (1999) applied the Schwinger variational iterative method (SVIM, Lucchese *et al* 1982) combined with the distorted-wave approximation (DWA, Lee and McKoy 1983, Lee *et al* 1990, 1993) to study the elastic electron scattering by the nitrogen molecule over a wide (20–800 eV) energy range. A complex optical interaction potential, derived from a fully molecular near-Hartree–Fock SCF wavefunction, was used to describe the electron–molecule interaction. In that work, QFSM version 3 was applied to generate the imaginary absorption potential. The comparison between the calculated cross sections and experimental results available in the literature is very encouraging. Since the validity of a theoretical model can only be established through extensive and systematic investigations for various targets over a wide energy range, in this work, the referred complex optical potential is applied to the studies of electron collision on

CO_2.

In the present investigation, we report a joint theoretical and experimental study on electron scattering by CO_2 in the intermediate energy range. More specifically, the calculated elastic DCS, ICS, MTCS and TCS at electron impact energies ranging from 20–500 eV as well as measured DCS in the 100–400 eV range are presented.

The organization of this paper is as follows. In section 2, we describe briefly the theory used and also some details of the calculation. In section 3 we present briefly some experimental details. Finally, in section 4 we compare our calculated results with our and the existing experimental data and with some other theoretical data available in the literature.

2. Theory and calculation

Since the details of the SVIM and the DWA have already been presented in previous works, here we will only outline briefly the theory used. After carrying out the average over the molecular orientation, the j_t basis representation (Fano and Dill 1972) of the laboratory-frame (LF) DCS for elastic electron–CO_2 scattering is given by

$$\frac{\mathrm{d}\sigma}{\mathrm{d}\Omega} = \frac{\pi}{k^2} \sum_{j_t m_t m_t'} \frac{1}{(2j_t+1)} \left| B^{j_t}_{m_t m_t'} \right|^2 \tag{1}$$

where k is the magnitude of the linear momentum of the incoming electron, $\vec{j}_t = \vec{l}' - \vec{l}$, the transferred angular momentum during the collision with projections m_t' and m_t along the laboratory and molecular axes, respectively. In equation (1), $B^{j_t}_{m_t m_t'}$ is the coefficient of the j_t-basis expansion of the LF scattering amplitudes and is given by

$$B^{j_t}_{m_t m_t'}(\Omega') = \sum_{l'lm'm} (-1)^m a_{ll'mm'} \left(ll'0m_t \middle| j_t m_t\right) \left(ll'mm' \middle| j_t m_t'\right) Y_{lm_l}(\Omega') \tag{2}$$

where the dynamical coefficients $a_{ll'mm'}$ are related to the partial-wave components of the elastic T-matrix as

$$a_{ll'mm'} = -\tfrac{1}{2}\pi [4\pi(2l'+1)]^{1/2} \mathrm{i}^{l'-l} \langle k_n lm, n|T|k_0 l' - m, 0\rangle. \tag{3}$$

The elastic scattering T-matrix is calculated using a complex optical potential, given by

$$V_{\mathrm{opt}}(\vec{r}) = V^{\mathrm{SEP}}(\vec{r}) + \mathrm{i} V_{ab}(\vec{r}) \tag{4}$$

where the V^{SEP} is the real part of the interaction potential formed by the static, the exchange and the correlation–polarization contributions as

$$V^{\mathrm{SEP}}(\vec{r}) = V_{\mathrm{st}}(\vec{r}) + V_{\mathrm{ex}}(\vec{r}) + V_{\mathrm{cp}}(\vec{r}) \tag{5}$$

and V_{ab} is the absorption potential. In our calculation, V_{st} and V_{ex} are treated exactly, while V_{cp} is obtained within the framework of the free-electron-gas model derived from a parameter-free local density, as prescribed by Padial and Norcross (1984). The same dipole polarizabilities adopted by Takekawa and Itikawa (1996), $\alpha_0 = 17.84$ au and $\alpha_2 = 8.80$ au, were used to calculate the asymptotic form of V_{cp}. The absorption potential V_{ab} in equation (4) is given by (Staszewska *et al* 1984):

$$V_{ab}(\vec{r}) = -\rho(\vec{r})(T_L/2)^{1/2} \left(8\pi/5k^2k_{\mathrm{F}}^3\right) H\left(\alpha + \beta - k_{\mathrm{F}}^2\right)(A + B + C) \tag{6}$$

where

$$T_L = k^2 - V^{\mathrm{SEP}} \tag{7}$$

$$A = 5k_{\mathrm{F}}^3/\left(\alpha - k_{\mathrm{F}}^2\right) \tag{8}$$

$$B = -k_{\mathrm{F}}^3\left(5\left(k^2 - \beta\right) + 2k_{\mathrm{F}}^2\right)/\left(k^2 - \beta\right)^2 \tag{9}$$

and

$$C = 2H\left(\alpha + \beta - k^2\right)\frac{\left(\alpha + \beta - k^2\right)^{5/2}}{\left(k^2 - \beta\right)^2}. \tag{10}$$

In equations (6)–(10), k_{F} is the Fermi momentum and $\rho(\vec{r})$ is the local electronic density of the target. $H(x)$ is a Heaviside function defined by $H(x) = 1$ for $x \geqslant 0$ and $H(x) = 0$ for $x < 0$. According to QFSM version 3 of Staszewska *et al* (1984),

$$\alpha(\vec{r}, E) = k_{\mathrm{F}}^2 + 2(2\Delta - I) - V^{\mathrm{SEP}} \tag{11}$$

and

$$\beta(\vec{r}, E) = k_{\mathrm{F}}^2 + 2(I - \Delta) - V^{\mathrm{SEP}} \tag{12}$$

where Δ is the mean excitation energy and I is the ionization potential. In this study, the published ionization potential $I = 0.5071$ au (Jain and Baluja 1992) is used and the mean excitation energy of the target is assumed to be the same as I as suggested by Jain and Baluja (1992).

To proceed, the interaction potential is split into

$$V_{\mathrm{opt}} = U_1 + U_2 \tag{13}$$

where U_1 is taken as the real part of the complex optical potential, whereas U_2 is the imaginary absorption potential. The corresponding distorted wavefunctions satisfy the following scattering equation:

$$(H_0 + U_1 - E)\chi = 0 \tag{14}$$

which is solved using the SVIM (Lucchese *et al* 1982). Furthermore, the absorption part of the T-matrix is calculated via DWA as

$$T_{ab} = \mathrm{i}\langle\chi_f^- \big| V_{ab} \big| \chi_i^+\rangle. \tag{15}$$

In the SVIM calculations, the continuum wavefunctions are single-centre expanded as

$$\chi_{\vec{k}}(\vec{r}) = (2/\pi)^{1/2}\sum_{lm}\frac{(\mathrm{i})^l}{k}\chi_{klm}(\vec{r})Y_{lm}(\hat{k}) \tag{16}$$

where $Y_{lm}(\hat{k})$ are the usual spherical harmonics.

The calculation of $\chi_{\vec{k}}(\vec{r})$ starts with the expansion of the trial functions in a set R_0 of L^2-basis functions $\alpha_i(\vec{r})$ as follows:

$$\tilde{\chi}_{k,lm}(\vec{r}) \;=\; \sum_{i=1}^{N} a_{i,lm}(k)\,\alpha_i(\vec{r}). \tag{17}$$

Using this basis set, the reactance K-matrix elements can be derived as

$$K_{k,ll'm}^{(R_0)} \;=\; \sum_{i,j=1}^{N}\langle\Phi_{k,l'm}\big|U_1\big|\alpha_i\rangle\left[D^{-1}\right]_{ij}\langle\alpha_j\big|U_1\big|\Phi_{k,lm}\rangle \tag{18}$$

where $\Phi_{k,lm}$ are the partial-wave free-particle wavefunctions and

$$D_{ij} = \langle \alpha_i | U_1 - U_1 G_0^{(P)} U_1 | \alpha_j \rangle \tag{19}$$

where $G_0^{(\mathrm{P})}$ is the principal value of the free-particle Green's operator and the zeroth-iteration wavefunction $\chi_{k,lm}^{R_0}$ is calculated using equation (20) with appropriately calculated coefficients $a_{i,lm}$. As demonstrated by Lucchese *et al* (1982), the converged scattering solutions can be obtained via an iterative procedure. This procedure consists in augmenting the basis set R_0 by the set

$$S_0 = \left\{ \chi_{k,l_1 m_1}^{(P)^{(R_0)}}(\vec{r}),\ \chi_{k,l_2 m_2}^{(P)^{(R_0)}}(\vec{r}),\ \ldots,\ \chi_{k,l_c m_c}^{(P)^{(R_0)}}(\vec{r}) \right\} \tag{20}$$

where l_c is the maximum value of l for which the expansion of the scattering solution (19) is truncated, and $m_c \leqslant l_c$. A new set of partial-wave scattering solutions can now be obtained from

$$\chi_{k,lm}^{(P)^{(R_1)}}(\vec{r}) \ = \ \Phi_{k,lm}(\vec{r}) + \sum_{i,j=1}^{M} \langle \vec{r} | G^{(P)} U_1 | \eta_i^{(R_1)} \rangle \left[D^{-1} \right]_{ij} \langle \eta_j^{(R_1)} | U_1 | \Phi_{k,lm} \rangle \tag{21}$$

where $\eta_i^{(R_1)}(\vec{r})$ is any function in the set $R_1 = R_0 \cup S_0$ and M is the number of functions in R_1. This iterative procedure continues until a converged $\chi_{k,lm}^{(P)^{(R_n)}}(\vec{r})$ is achieved. In the present calculations, three iterations are needed to obtain the converged scattering functions.

The SCF wavefunction of CO_2 is derived at the equilibrium geometry with the (C–O) distance as 2.191 69 au. The basis set used for this calculation is published in one of our early studies for CO (Lee *et al* 1996). With this basis set, the obtained total energy is -187.6965 au, in good agreement with the calculated values of -187.7140 au (Takekawa and Itikawa 1996) and -187.7014 au (Tanaka *et al* 1998).

All matrix elements appearing in the present calculations were computed by a single-centre expansion technique with the radial integral evaluated using a Simpson quadrature. The contributions from the direct and exchange parts were truncated at $l = 58$ and 40, respectively. In the SVIM calculations, we have limited the partial-wave expansions up to $l_{\max} = 40$ and $m_{\max} = 17$. Furthermore, contributions from the higher partial waves were accounted for via the Born-closure procedure, where the $B_{m_t m_t'}^{j_t}$ is given by

$$B_{m_t m_t'}^{j_t}(\hat{k}') = B_{m_t m_t'}^{\mathrm{Born},\, j_t}(\hat{k}') + \sum_{l' l m m'} (-1)^m (\mathrm{i})^{l-l'} (2l+1)^{-1} \left(T_{ll'mm'}^{S} - T_{ll'mm'}^{\mathrm{Born}} \right)$$
$$\times \left(l - m, l' m' | j_t' m_t' \right) \left(l 0, l' m_t | j_t m_t \right) Y_{l' m_t}(\hat{k}'). \tag{22}$$

In equation (22), $B_{m_t m_t'}^{\mathrm{Born},\, j_t}|(\hat{k}')$ is the j_t-basis representation of the Born scattering amplitude, defined as

$$B_{m_t m_t'}^{\mathrm{Born},\, j_t}(\hat{k}') = \frac{(2j_t + 1)}{8\pi^2} \frac{k}{\mathrm{i}\pi^{(1/2)}} \int \mathrm{d}\hat{R}'\, f^{\mathrm{Born}}\left(\hat{R}'; \hat{k}'\right) D_{m_t m_t'}^{j_t *}\left(\hat{R}'\right) \tag{23}$$

where $D_{m_t m_t'}^{j_t *}(\hat{R}')$ are the usual rotation matrices and $T_{ll'mm'}^{\mathrm{Born}}$ is the partial-wave Born T-matrix element given by

$$T_{ll'mm'}^{\mathrm{Born}} = \langle \Phi_{klm} | U_{\mathrm{st}} | \Phi_{kl'm'} \rangle. \tag{24}$$

Moreover, the total cross sections for electron–molecule scattering are obtained using the optical theorem, namely

$$\sigma_{\mathrm{tot}} = \frac{4\pi}{k} \operatorname{Im} f_{\mathrm{el}}(\theta = 0^{\circ}) \tag{25}$$

where f_{el} is the scattering amplitude for elastic electron–molecule collisions.

3. Experimental

Details of our experimental set-up and procedure will be presented elsewhere (Homem and Iga 1999) and thus will only be presented briefly here. Our spectrometer, a crossed-beam apparatus, is built inside a vacuum chamber pumped by a 6 in diffusion pump. The typical background pressure (no gas load) in the vacuum chamber is about 1×10^{-7} torr. Three pairs of Helmholtz coils around the chamber reduce the magnetic field in the collision region to less than 15 mG.

The electron gun used is of a simple design, composed by a hairpin tungsten filament, a triode extraction, a set of einzel lenses and two sets of electrostatic deflectors in the x, y directions, respectively. The electron beam is generated without prior energy selection. A typical beam current in the 100–1000 eV range is around 1 μA with a diameter of 1 mm. The energy resolution of the electron beam is about 0.5 eV. Perpendicular to the electron beam, a molecular beam flows into the vacuum chamber via a capillary array. This array has an external diameter of 1 mm with individual capillaries of diameter (D) 0.05 mm and length (L) 5 mm (aspect ratio $\gamma = D/L = 0.01$). Intensities of scattered electrons are collected in the angular range covered from 5° to 135° and −5° to −60°. A pair of apertures of diameter 1 mm in the detector/analyser system limits the viewcone of the detector and the resulting angular resolution is about 0.2°. The scattered electrons are energy filtered by a retarding-field energy selector (RFES). The resolution of the RFES is about 1.5 eV for an incident energy of 500 eV. With this resolution, it is sufficient to discriminate inelastically scattered electrons resulting from electronic excitation for most small molecules, but nevertheless is unable to separate those from vibrational excitation processes. After being energy analysed, the elastically scattered electrons are detected by a channeltron.

During the measurement, the working pressure in the vacuum chamber is around 5×10^{-7} torr with the gas beam turned on. For each scattering angle and incident energy, the scattering intensities are recorded at least three times. The counting time is monitored to ensure that the statistical deviation of counts is less than 3%. Also the electrons scattered by background gases are measured. In this case, the gas beam from the capillary array is interrupted and the gas is allowed to flow into the chamber via a side leak far from the collision region and the scattering intensities are recorded. These background contributions are subtracted from the scattering intensities for each angle.

It is well known that electron–molecule collisions in the intermediate energy range may result in a variety of charged and neutral molecular fragments. Ultraviolet (UV) photons can also be generated via a radiative decay process from excited molecules. Although the potentials applied at RFES and at the channeltron cone during the measurements prevent both positively and negatively charged molecular fragments from reaching the detector, it has no effect on UV photons or neutral fragments. Therefore, their contributions are measured and subsequently subtracted from the scattering intensities. For that, polarities of the potentials applied at the RFES and channeltron cone are inverted. It is found that the contribution of these species is negligible.

The recorded scattering intensities are converted into absolute elastic DCS using the relative flow technique (RFT). The RFT has been used widely (Srivastava *et al* 1975, Brinkman and Trajmar 1981, Khakoo and Trajmar 1986, Nickel *et al* 1989, Brunger *et al* 1991, Alle *et al* 1992, Khakoo *et al* 1993, Tanaka *et al* 1998) in measurements of electron–atom (molecule) collisional cross sections. This technique bypasses the determination of many experimental parameters required for an absolute measurement of the cross sections by comparing the scattering intensities of the gas under study (x) with those of a reference gas (std) of known DCS, under identical experimental conditions, i.e.

$$(\mathrm{DCS})_x = (\mathrm{DCS})_{\mathrm{std}} \frac{I_x}{I_{\mathrm{std}}} \frac{n_{\mathrm{std}}}{n_x} \left(\frac{M_{\mathrm{std}}}{M_x} \right)^{1/2} \tag{26}$$

where I is the scattered electron intensity, n is the flow rate and M is the molecular weight. The above equation is valid if the beam profiles (density distribution) of both gases, x and std, are nearly the same. According to Olander and Kruger (1970), this requirement is fulfilled under two conditions: equal mean free paths (λ) of the gases behind the capillaries or with the Knudsen number K_L defined as λ/L of the beam flow varying between $\gamma \leqslant K_L \leqslant 10$.

Recently, the applicability of RFT to absolute cross section determinations has been discussed extensively (Buckman *et al* 1993, Khakoo *et al* 1993, Sagara and Boesten 1998, Tanaka *et al* 1998). Several studies (Buckman *et al* 1993, Tanaka *et al* 1998) have shown that even at beam flow regimes where the K_Ls are significantly lower than γ, the density distributions of most gases measured in their works can still be very similar to each other. In particular, a systematic study regarding the influences of the secondary standards as well as the range of working pressure was carried out recently by our group (Homem and Iga 1999). It was shown that at flow conditions where $0.002 \leqslant K_L \leqslant \gamma$, reliable DCS for elastic e^-–N_2 scattering in the 300–500 eV range are obtained using the CH_4, Ne, Ar and Kr as secondary standards. In some manner, our findings agree with the study carried out by Buckman *et al* (1993). In that work, the authors have reported that the profiles (FWHM) of the gaseous beams of several gases heavier than He are about the same even at flow conditions with K_L values significantly lower than γ.

In the present study, N_2 is used as the reference gas. The collisional diameters of N_2 and CO_2 are 3.14 (Roth 1982) and 4.53 Å (Tanaka *et al* 1998), respectively, and thus the theoretical pressure ratio for equal Knudsen numbers would be 2.1:1. We used 5 torr for N_2 and 2.4 torr for CO_2. This corresponds to a mean free path of 14.2 μm and $K_L = 0.0028$ for both gases. In addition, the absolute cross sections of Jansen *et al* (1976) for N_2 are used for normalization of our data.

Besides the uncertainties due to the normalization procedure, errors of a random nature such as fluctuations of the primary electron beam current, pressure fluctuations, etc, contribute to the overall experimental errors of the measured data. In our experiments, the uncertainty due to pressure fluctuations is less than 0.2%, the accuracy of the measurements of electron beam current is better than 1%, errors due to the uncertainties in scattering-angle reading are estimated as 1% and the error due to background scattering is less than 1%. These contributions combined with the estimated statistical error of 3% give an overall error of 4% on the relative DCS for each gas. Moreover, the quoted error on the absolute DCS of Jansen *et al* (1976) is 6.5%. In addition, the experimental uncertainty associated with the normalization procedure is estimated to be 5.7%. Therefore, the overall experimental uncertainty on our absolute DCS is about 10.3%.

In order to obtain the ICS and MTCS, DCS of limited angular range have to be extrapolated both at low and high angles. A manual extrapolation procedure was carried out, following the trends of the measured DCS of Bromberg (1974) at small scattering angles and the present

calculated DCS at large scattering angles. The uncertainties of this procedure are estimated to be 10% at small angles and 20% at large angles, which lead to overall errors of 18% in ICS and 20% in MTCS.

4. Results and discussion

In figures 1–3 we present our calculated DCS in the 30–100 eV range along with some available measured data (Register *et al* 1980, Kanik *et al* 1989, Tanaka *et al* 1998). Some

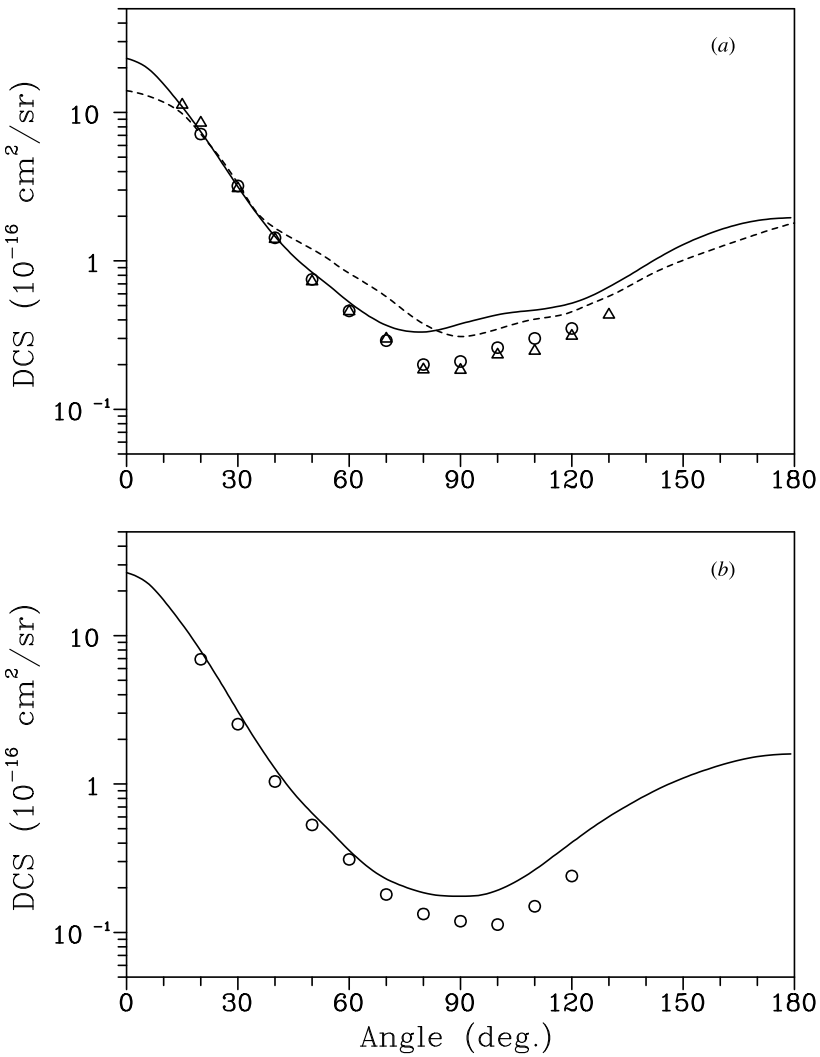

Figure 1. Elastic differential cross sections for e^-–CO_2 scattering at (*a*) 30 eV, (*b*) 40 eV. Full curve, present calculated results; short-broken curve, calculated results of Takekawa and Itikawa (1996); open circles, experimental data of Kanik *et al* (1989); open triangles, experimental data of Tanaka *et al* (1998).

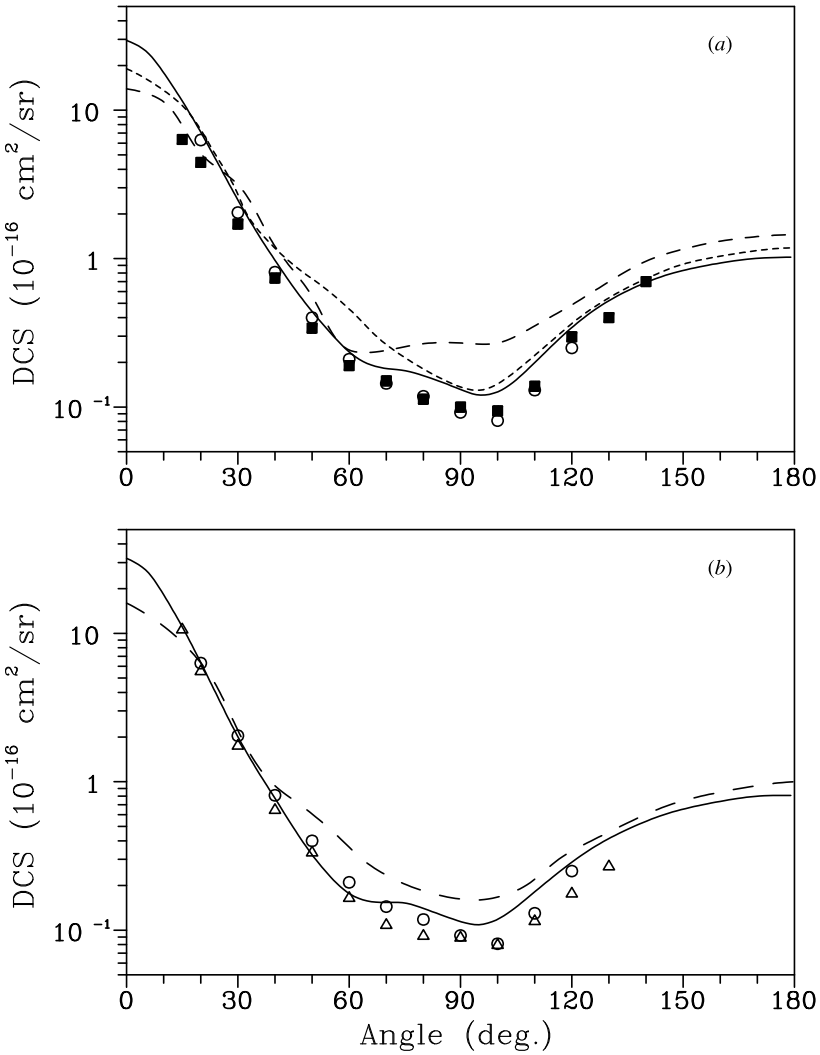

Figure 2. Same as figure 1 at (*a*) 50 eV, (*b*) 60 eV except: broken curve, calculated results of Tanaka *et al* (1998); long-broken curve, calculated results of Gianturco and Stoecklin (1996); full squares, experimental data of Register *et al* (1980).

recent calculated results (Takekawa and Itikawa 1996, Gianturco and Stoecklin 1996, Tanaka *et al* 1998) are also shown for comparison. In general, our calculated results are in very good agreement, both in shape and magnitude, with the experimental data, particularly at incident energies $E_0 \geqslant 50$ eV. Also, the comparison with the existing theoretical results has shown a very good qualitative agreement among each other in the entire overlapping energy range. Quantitatively, however, the existing calculated results used overestimate the DCS significantly at intermediate and large scattering angles. This overestimate of the DCS is somewhat expected since no absorption effects were accounted for in those calculations. It is well known that at impact energies above excitation and ionization thresholds, the flux of the scattered electrons is distributed over all the open channels,

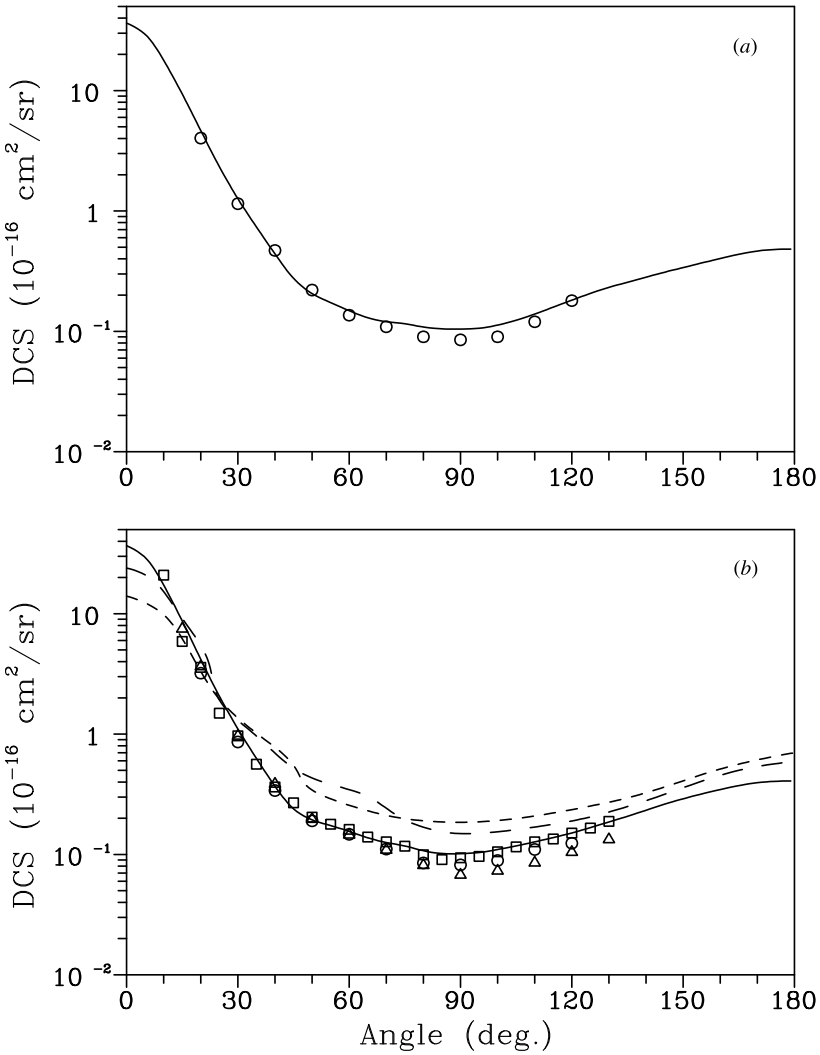

Figure 3. Same as figure 2 at (*a*) 90 eV, (*b*) 100 eV except: open squares, present measured data.

consequently resulting in a reduction of the flux corresponding to the elastic scattering. Even at 30 eV where the influence of the absorption effects is expected to be small, the inclusion of these effects into calculations can still improve the agreement between theoretical and measured cross sections. Further, our measured data at 100 eV also agree very well with some earlier data (Kanik *et al* 1989, Tanaka *et al* 1998) and with the present calculated DCS.

Above 100 eV, there are no other theoretical results reported in the literature. Therefore, in figures 4 and 5 we compare our calculated DCS in the 200–500 eV range with the presently measured data and with some previously reported experimental results (Bromberg 1974, Iga *et al* 1987). Again a very good agreement, both in shape and magnitude, between the theory and experiments is seen. Also, our measured data are in good agreement with those reported by Bromberg (1974) in the overlapping energy and angular ranges.

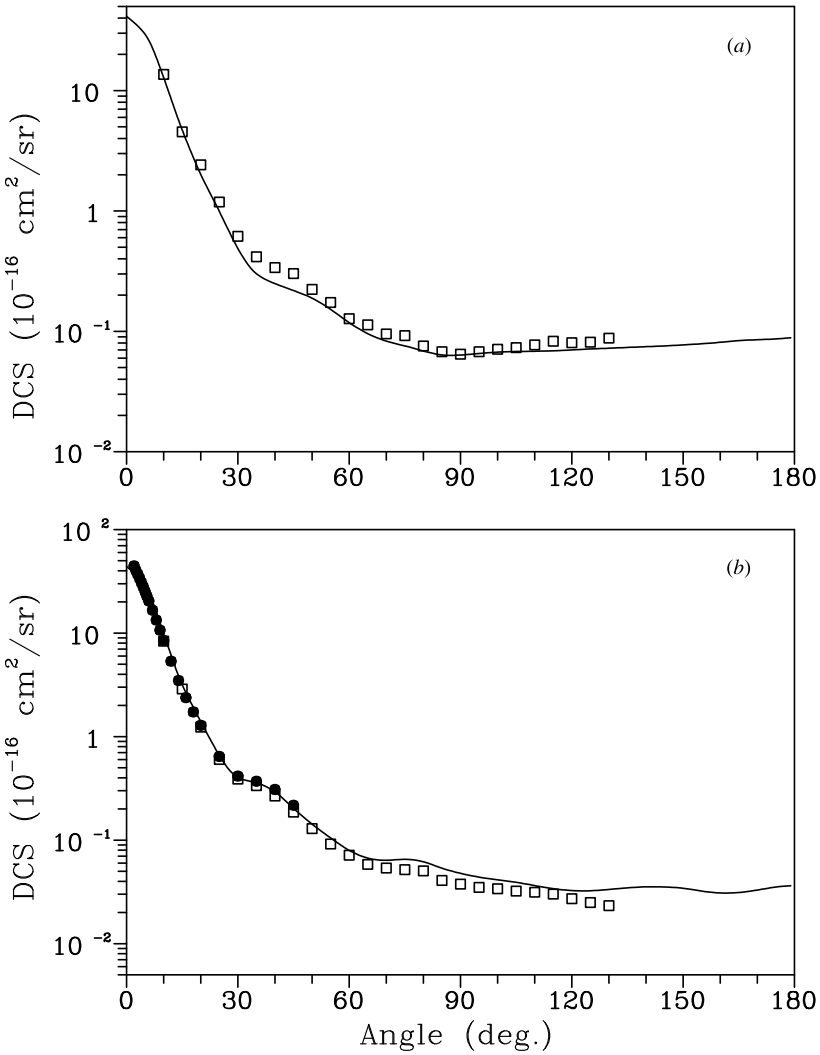

Figure 4. Same as figure 3 at (*a*) 200 eV, (*b*) 300 eV except: full circles, measured data of Bromberg (1974).

In figure 6, we compare our calculated ICS and MTCS in the 20–500 eV range with the available calculated (Jain and Baluja 1992, Takekawa and Itikawa 1996, Gianturco and Stoecklin 1996, Tanaka *et al* 1998) and measured (Register *et al* 1980, Tanaka *et al* 1998, Iga *et al* 1984, Nakamura 1995) data reported in the literature. The present measured data of ICS and MTCS in the 100–400 eV range are also shown for comparison. Our calculated and measured ICS and MTCS agree very well with each other. Good agreement is also seen between our calculated results with available experimental results and with the calculated data of Takekawa and Itikawa (1996) and Gianturco and Stoecklin (1996) in the overlapping energy range. Nevertheless, the calculation of Jain and Baluja (1992) strongly overestimates the ICS in the entire energy range covered herein. This discrepancy is somehow expected since in their calculation, only the spherical parts of the interaction potentials were used to describe

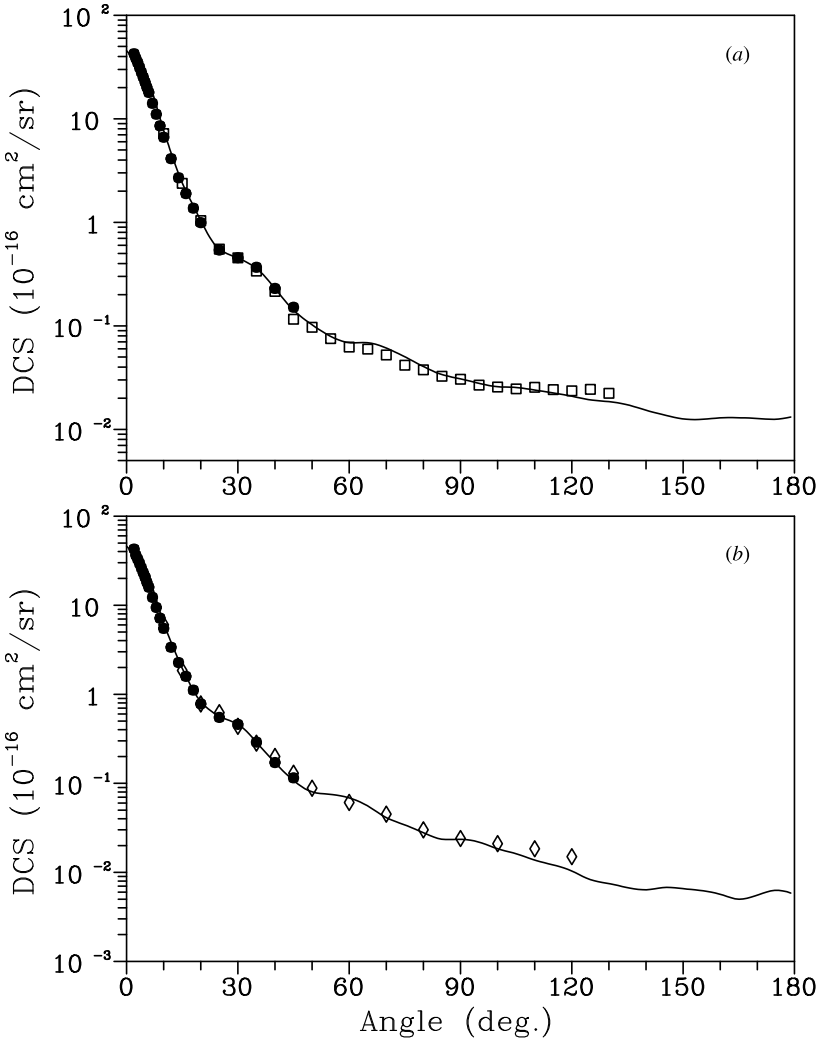

Figure 5. Same as figure 4 at (*a*) 400 eV, (*b*) 500 eV except: open diamonds, measured data of Iga *et al* (1984).

the electron–CO_2 scattering. Although the spherical approach may work reasonably well for highly symmetric molecules such as CH_4, SiH_4 and SF_6, etc, it will certainly not work for a highly anisotropic molecule such as CO_2. The neglect of the non-spherical contributions of the interaction potentials, particularly the static potential, is certainly too drastic and could be the origin of the disagreement between their calculated ICS and experiments, mainly at the low incident energies.

Figure 7 compares our calculated TCS with the available experimental (Hoffmann *et al* 1982, Kwan *et al* 1983, Sueoka and Mori 1984, Szmytkowski *et al* 1987) and calculated data (Jain and Baluja 1992) reported in the literature. Our TCS are in general good agreement with the measured data for incident energies below 100 eV. Above that energy, our calculation systematically underestimates the TCS: about 10% lower than the measured data reported by Sueoka and Mori (1984) and 20% lower than those of Kwan *et al* and Szmytkowski *et al*. This

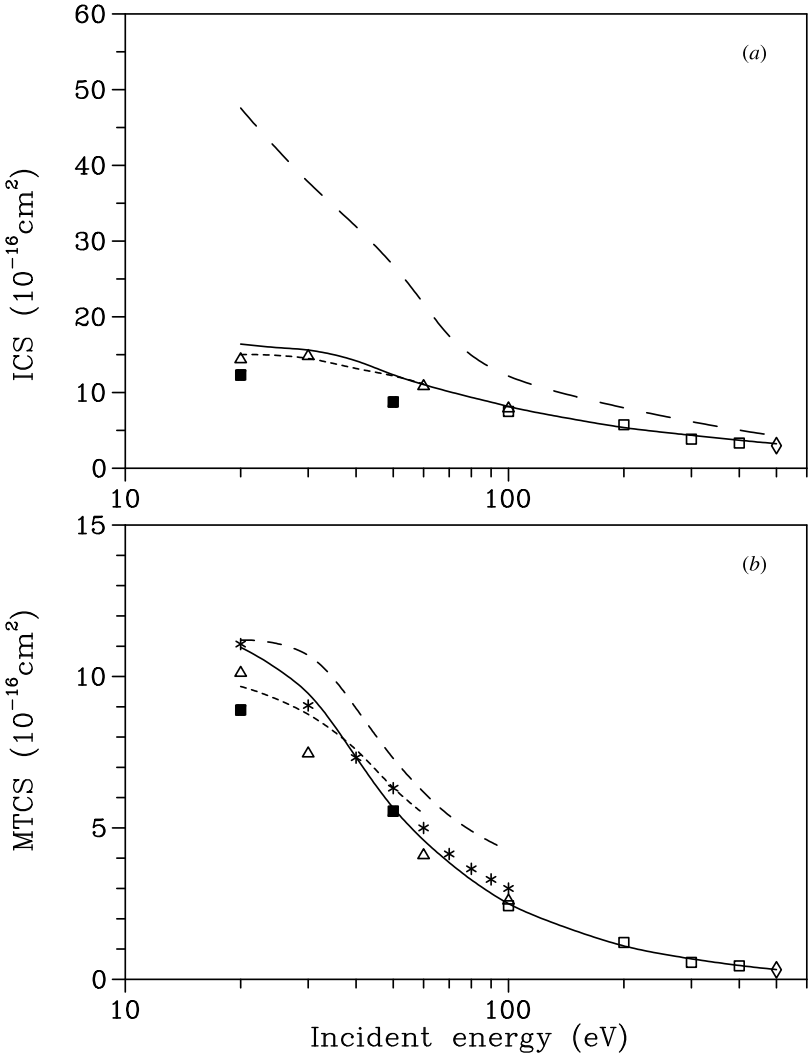

Figure 6. (*a*) ICS and (*b*) MTCS for elastic electron scattering by CO_2 in the 20–500 eV range. Full curve, present calculated results; short-broken curve, calculated results of Takekawa and Itikawa (1996); broken curve, calculated results of Gianturco and Stoecklin (1996); long-broken curve, calculated results of Jain and Baluja (1992); open triangles, experimental data of Tanaka *et al* (1998); stars, experimental results of Nakamura (1995); full squares, experimental data of Register *et al* (1980); open squares, present measured data; open diamonds, measured data of Iga *et al* (1984).

agreement is still satisfactory considering the simplicity of the theoretical model used for the description of the interaction between an electron and a complex molecule like CO_2. Again, the calculated results of Jain and Baluja (1992) strongly disagree with our calculated results and experimental data.

For the sake of completeness, the measured DCS, ICS and MTCS for elastic e^-–CO_2 scattering in the 100–400 eV range are presented in table 1.

In summary, in this work we report a joint theoretical and experimental investigation on electron–CO_2 scattering over a wide energy range. A complex optical potential composed of an

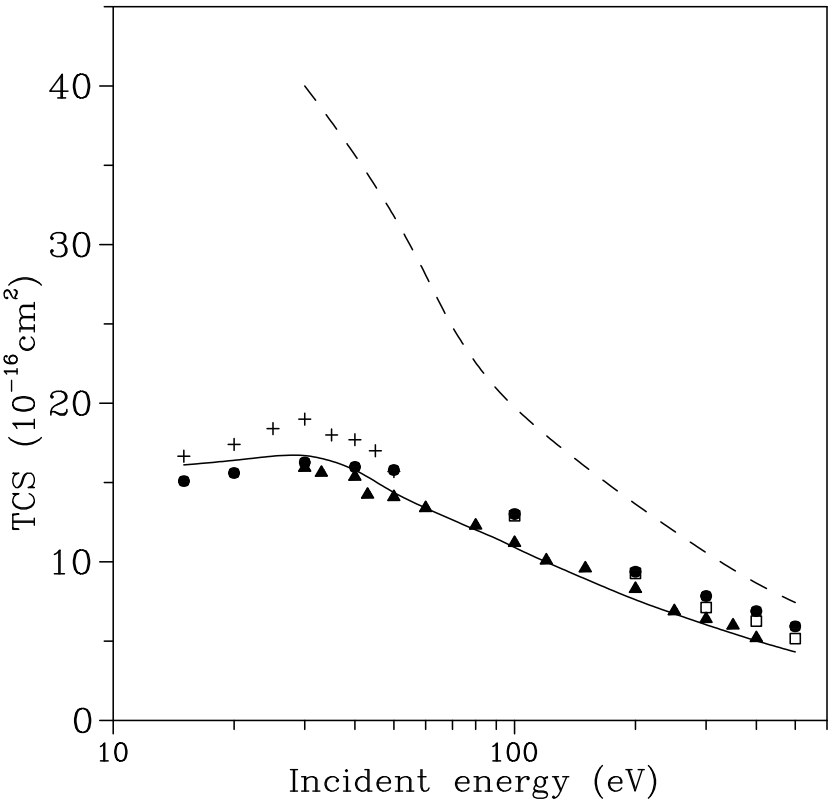

Figure 7. TCS for electron scattering by CO_2 in the 20–500 eV range. Full curve, present calculated results; long-broken curve, calculated results of Jain and Baluja (1992); open squares, measured data of Kwan *et al* (1983); full triangles, measured TCS of Sueoka and Mori (1984); full circles, measured data of Szmytkowski *et al* (1987); crosses, experimental data of Hoffmann *et al* (1982).

exact static-exchange contribution plus a parameter-free FEG model correlation–polarization and absorption contributions are used to calculated elastic DCS, ICS and MTCS as well as the TCS. The present investigation shows that the absorption phenomena play a very important role for electron–CO_2 molecule collisions at the intermediate incident energies and should be taken into account. In particular, the good agreement between the present calculated DCS, ICS and MTCS and experimental data for elastic electron–CO_2 collisions in the 30–500 eV range is very encouraging. On the other hand, our calculated TCS using QFSM version 3 lie systematically about 10–20% below the experimental results in the 100–500 eV range. This agreement is still acceptable considering the simplicity of the model V_{ab} used in the calculations.

In addition, due to the scarceness of experimental data for elastic electron–CO_2 scattering above 100 eV, we have also measured DCS, ICS and MTCS for this molecule in the 100–400 eV range. Our measured DCS are in very good agreement with the limited experimental data available in the literature at the overlapping energies and scattering angles. Very good agreement is also seen between our calculated and measured results in the entire energy range covered herein.

In view of the success achieved in the present investigation, in particular for elastic electron–molecule scattering, as well as the need for the cross sections for these processes in

Table 1. Experimental DCS, ICS and MTCS (in 10^{-16} cm^2) for elastic e^-–CO_2 scattering.

Angle (deg)	E_0 (eV)			
	100	200	300	400
10	20.93	13.61	8.372	7.190
15	5.880	4.539	2.885	2.377
20	3.580	2.417	1.235	1.040
25	1.490	1.186	0.601	0.550
30	0.967	0.616	0.388	0.455
35	0.562	0.416	0.336	0.338
40	0.363	0.338	0.267	0.215
45	0.268	0.301	0.186	0.116
50	0.204	0.223	0.129	0.0968
55	0.178	0.174	0.0917	0.0752
60	0.162	0.127	0.0716	0.0624
65	0.140	0.113	0.0583	0.0596
70	0.127	0.0952	0.0539	0.0523
75	0.117	0.0921	0.0519	0.0418
80	0.0992	0.0756	0.0505	0.0376
85	0.0908	0.0676	0.0408	0.0325
90	0.0938	0.0646	0.0376	0.0305
95	0.0964	0.0676	0.0350	0.0268
100	0.105	0.0709	0.0337	0.0256
105	0.115	0.0732	0.0323	0.0246
110	0.126	0.0770	0.0314	0.0255
115	0.135	0.0827	0.0302	0.0242
120	0.150	0.0804	0.0272	0.0236
125	0.166	0.0812	0.0249	0.0244
130	0.188	0.0878	0.0233	0.0223
ICS	7.50	5.74	3.84	3.33
MTCS	2.43	1.22	0.56	0.44

several fields of application, the extension of such joint theoretical–experimental investigations to other molecular targets is certainly of interest. Some such studies are underway.

Acknowledgments

This work is partially supported by Brazilian agencies FINEP-PADCT, CNPq and FAPESP.

References

Alle D T, Gulley R J, Buckman S J and Brunger M J 1992 *J. Phys. B: At. Mol. Opt. Phys.* **25** 1533
Botelho L F, Freitas L C G, Lee M-T, Jain A and Tayal S S 1984 *J. Phys. B: At. Mol. Phys.* **17** L641
Brinkman R T and Trajmar S 1981 *J. Phys. E: Sci. Instrum.* **14** 245
Bromberg J P 1974 *J. Chem. Phys.* **60** 1717
Brunger M J, Buckman S J, Newman D J and Alle D T 1991 *J. Phys. B: At. Mol. Opt. Phys.* **24** 1435
Buckman S J, Gulley R J, Moghbelalhossein M and Bennett S J 1993 *Meas. Sci. Technol.* **4** 1143
Collins L A and Morrison M A 1982 *Phys. Rev.* A **25** 1764
Fano U and Dill D 1972 *Phys. Rev.* A **6** 185
Ferch J, Masche C and Raith W 1981 *J. Phys. B: At. Mol. Phys.* **14** L97
Gianturco F A and Lucchese R R 1996 *J. Phys. B: At. Mol. Opt. Phys.* **29** 3955
Gianturco F A and Stoecklin T 1996 *J. Phys. B: At. Mol. Opt. Phys.* **29** 3933

Green A E S, Rio D E and Ueda T 1981 *Phys. Rev.* A **24** 3010
Hoffman K R, Dababneh M S, Hsieh Y-F, Kauppila W E, Pol V, Smart J H and Stein T S 1982 *Phys. Rev.* A **25** 1393
Homem M G P and Iga I 1999 to be published
Iga I, Nogueira J C and Lee M-T 1984 *J. Phys. B: At. Mol. Phys.* **17** L185
Jain A 1986 *Phys. Rev.* A **34** 3707
Jain A and Baluja K L 1992 *Phys. Rev.* A **45** 202
Jansen R H J, de Heer F J, Luyken H J, von Wingerden B and Blaauw H J 1976 *J. Phys. B: At. Mol. Phys.* **9** 185
Jiang Y, Sun J and Wan L 1995 *Phys. Rev.* A **52** 398
Joachain C 1983 *Quantum Collision Theory* (Amsterdam: North-Holland)
Joachain C J, Vanderpoorten K H, Winters K H and Byron F W Jr 1977 *J. Phys. B: At. Mol. Phys.* **10** 227
Kanik I, McCollum D C and Nickel J C 1989 *J. Phys. B: At. Mol. Opt. Phys.* **22** 1225
Khakoo M A, Jayawera T, Wang S and Trajmar S 1993 *J. Phys. B: At. Mol. Opt. Phys.* **26** 4845
Khakoo M A and Trajmar S 1986 *Phys. Rev.* A **34** 138
Kwan Ch K, Hsieh Y-F, Kauppila W E, Smith S J, Stein T S, Uddin M N and Dababneh M S 1983 *Phys. Rev.* A **27** 1328
Lee M-T, Brescansin L M and Lima M A P 1990 *J. Phys. B: At. Mol. Opt. Phys.* **23** 3859
Lee M-T and Iga I 1999 *J. Phys. B: At. Mol. Opt. Phys.* **32** 453
Lee M-T, Machado A M, Fujimoto M M, Machado L E and Brescansin L M 1996 *J. Phys. B: At. Mol. Opt. Phys.* **29** 2113
Lee M-T and McKoy V 1983 *Phys. Rev.* A A **28** 697
Lee M-T, Michelin S, Machado L E and Brescansin L M 1993 *J. Phys. B: At. Mol. Opt. Phys.* **23** 4331
Lucchese R R and McKoy V 1982 *Phys. Rev.* A **25** 1963
Lucchese R R, Raseev G and McKoy V 1982 *Phys. Rev.* A **25** 2572
Lynch M G, Dill D, Siegel J and Dehmer J L 1979 *J. Chem. Phys.* **71** 4249
McCarthy I E, Noble C J, Philips B A and Turnbull A D 1977 *Phys. Rev.* A **15** 2173
Morrison M A, Lane N F and Collins L A 1977 *Phys. Rev.* A **15** 2186
Nakamura Y 1995 *Aust. J. Phys.* **48** 357
Nickel J C, Zetner P W, Shen G and Trajmar S 1989 *J. Phys. E: Sci. Instrum.* **22** 730
Olander D R and Kruger V 1970 *J. Appl. Phys.* **41** 2769
Onda K and Truhlar D G 1979 *J. Phys. B: At. Mol. Phys.* **12** 283
Padial N T and Norcross D W 1984 *Phys. Rev.* A **29** 1742
Register D F, Nishimura H and Trajmar S 1980 *J. Phys. B: At. Mol. Phys.* **13** 1651
Roth A 1982 *Vacuum Technology* (Amsterdam: North-Holland)
Sagara T and Boesten L 1998 *J. Phys. B: At. Mol. Opt. Phys.* **31** 3455
Shyn T W, Sharp W E and Carignan G R 1978 *Phys. Rev.* A **17** 1855
Srivastava S K, Chutjian A and Trajmar S 1975 *J. Chem. Phys.* **63** 2659
Staszewska G, Schwenke D W, Thirumalai D and Truhlar D G 1983 *Phys. Rev.* A **28** 2740
Staszewska G, Schwenke D W and Truhlar D G 1984 *Phys. Rev.* A **29** 3078
Sueoka O and Mori S 1984 *J. Phys. Soc. Japan* **53** 2491
Szmytkowski C, Zecca A, Karwasz G, Oss S, Maciag K, Marinković B, Brusa R S and Grisenti R 1987 *J. Phys. B: At. Mol. Phys.* **20** 5817
Takekawa M and Itikawa Y 1996 *J. Phys. B: At. Mol. Opt. Phys.* **29** 4227
Tanaka H, Ishikawa T, Masai T, Sagara T, Boesten L, Takekawa M, Itikawa Y and Kimura M 1998 *Phys. Rev.* A **57** 1798
Thirumalai D and Truhlar D G 1982 *Phys. Rev.* A **26** 793